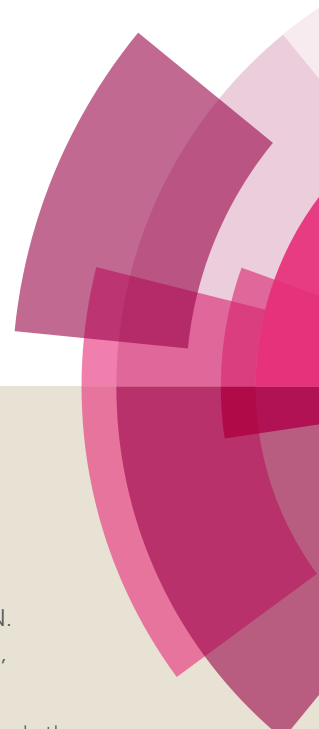


NJC

Accepted Manuscript



This article can be cited before page numbers have been issued, to do this please use: M. Alexandru, N. Marino, D. Visinescu, G. De Munno, M. Andruh, A. Bentama, F. Lloret and M. Julve, *New J. Chem.*, 2019, DOI: 10.1039/C9NJ00420C.



This is an Accepted Manuscript, which has been through the Royal Society of Chemistry peer review process and has been accepted for publication.

Accepted Manuscripts are published online shortly after acceptance, before technical editing, formatting and proof reading. Using this free service, authors can make their results available to the community, in citable form, before we publish the edited article. We will replace this Accepted Manuscript with the edited and formatted Advance Article as soon as it is available.

You can find more information about Accepted Manuscripts in the [author guidelines](#).

Please note that technical editing may introduce minor changes to the text and/or graphics, which may alter content. The journal's standard [Terms & Conditions](#) and the ethical guidelines, outlined in our [author and reviewer resource centre](#), still apply. In no event shall the Royal Society of Chemistry be held responsible for any errors or omissions in this Accepted Manuscript or any consequences arising from the use of any information it contains.

ARTICLE

A novel octacyanido dicobalt(III) building block for the construction of heterometallic compounds

Maria-Gabriela Alexandru,^{*a} Nadia Marino,^{*b} Diana Visinescu,^c Giovanni De Munno,^b Marius Andruh,^d Abdeslem Bentama,^e Francesc Lloret,^f and Miguel Julve^{*f}Received 00th January 20xx,
Accepted 00th January 20xx

DOI: 10.1039/x0xx00000x

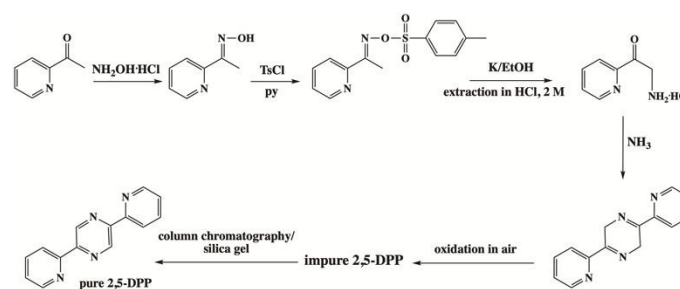
The first bimetallic octacyanido complex of Co^{III}, (PPh₄)₂[Co₂(μ-2,5-dpp)(CN)₈], (**1**), was synthesized and used as a metalloligand towards [Mn(MAC)(H₂O)₂]Cl₂·4H₂O to give a new {Co^{III}Mn^{II}} heterometallic chain of formula [Mn^{II}(MAC)(μ-NC)₂Co^{III}(μ-2,5-dpp)(CN)₆]_n·7nH₂O (**2**) (PPh₄⁺ = tetraphenylphosphonium cation; 2,5-dpp = 2,5-bis(2-pyridyl)pyrazine and MAC = 2,13-dimethyl-3,6,9,12,18-pentaazabicyclo-[12.3.1]octadeca-1(18),2,12,14,16-pentaene). Both compounds were characterized by single-crystal X-ray diffraction. Compound **1** contains a diamagnetic 2,5-dpp-bridged dicobalt(III) unit with four peripheral cyanide ligands at each cobalt center achieving a six-coordinate surrounding, the electroneutrality being ensured by bulky tetraphenylphosphonium cations. The structure of **2** consists of neutral heterobimetallic chains where the [Co₂(μ-2,5-dpp)(CN)₈]²⁻ complex anion adopts a bis-monodentate bridging mode towards the [Mn(MAC)]²⁺ cation. Each manganese(II) ion in **2** is seven-coordinate with five quasi coplanar nitrogen atoms from the macrocycle and two *trans*-positioned cyanide-nitrogen atoms building a somewhat distorted pentagonal bipyramidal environment. Cryomagnetic measurements for **2** reveal the occurrence of quasi magnetically isolated spin sextets in the temperature range 1.9-300 K.

Introduction

Polypyridyl-type ligands have been used as spacers towards transition metal ions to form polynuclear complexes with interesting structures and properties.¹ Exhaustive studies were performed on complexes of Ru^{II}, Os^{II}, Ir^{III} or Pt^{II} with pyridylpyrazine-type ligands focusing on their rich electrochemical and photophysical properties.^{1d,e,f,i} Some of these polydentate ligands induce spin crossover (SCO) phenomena in their Fe^{II} complexes.^{1g} Other examples with Ru^{II}, Rh^{III}, Ir^{III} and Au^{III} exhibit (photo)cytotoxic activity.^{1b,h,i} A special attention was also devoted to organometallic compounds of Ir^{III}, Ru^{II}, Ag^I, Re^I, Pt^{II}, etc.^{1j}

The organic compound 2,5-bis(2-pyridyl)pyrazine (2,5-dpp) represents an advantageous option as a ligand aiming at obtaining coordination compounds since it can act as a linker

towards transition metal ions. Examples of complexes with the 2,5-dpp molecule are still scarce, most likely because of the difficult synthetic route for this ligand.² In this respect, it deserves to be noted that the synthetic method used by Escuer *et al.* (first five steps in Scheme 1; yield 10%)^{2a} was improved by some of us (last step in Scheme 1; yield ca. 50%).^{2b} Recently, an alternative procedure to obtain this molecule published which is carried out under harder conditions (e.g. temperature of -78 °C) affords practically the same yield (ca. 55%).^{2c}



Scheme 1. Preparative route of 2,5-dpp.

Mononuclear complexes with 2,5-dpp were prepared and characterized especially with heavy metal ions such as Ru^{III}, Os^{III}, Cd^{II}.³ A tweezer molecule of Pt^{II} with 2,5-dpp, able to form heterobimetallic complexes was reported,⁴ as well as heteroleptic Ru^{II} polynuclear complexes⁵ and emissive Ir^{III} complexes.^{2c} There are also several examples of 2,5-dpp bridged hetero- and homometallic complexes are known. The photoluminescent {Cu^IRu^{II}} heterometallic species of formula [(bpy)₂Ru^{II}(μ-2,5-dpp)Cu^I(PPh₃)₂](PF₆)₅ is one example of the former ones.⁶ A series of binuclear complexes of divalent 3d

^a Department of Inorganic Chemistry, Physical Chemistry and Electrochemistry, Faculty of Applied Chemistry and Materials Science, University Politehnica of Bucharest, 1-7 Gh. Polizu Street, 011061 Bucharest, Romania. E-mail: alexandru.gabriela@gmail.com

^b Dipartimento di Chimica e Tecnologie Chimiche, Università della Calabria, 87036 Rende, Cosenza, Italy. E-mail: nadia.marino@unical.it

^c Coordination and Supramolecular Chemistry Laboratory, "Ilie Murgulescu" Institute of Physical Chemistry, Romanian Academy, Spaiul Independentei 202, Bucharest 060021, Romania

^d Inorganic Chemistry Laboratory, Faculty of Chemistry, University of Bucharest, Str. Dumbrava Rosie nr. 23, 020464, Bucharest, Romania.

^e Laboratoire de Chimie Organique Appliquée, Faculté des Sciences Techniques de Fès, Université Sidi Mohammed Ben Abdellah, Fès, Morocco

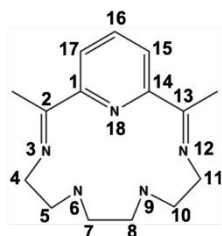
^f Departament de Química Inorgànica/Institut de Ciència Molecular (ICMol), Universitat de València, C/ Catedrático José Beltrán 2, 46990 Paterna, Valencia, Spain. E-mail: miguel.julve@uv.es.

† Electronic Supplementary Information (ESI) available: Infrared spectra [Figs. S1 (1) and S2 (2)] and tables of bond lengths and angles [Tabs. S1 (1) and S2 (2)]. CCDC 1892383 and 1892384 for complexes **1** and **2**, respectively. See DOI: 10.1039/x0xx00000x

metal ions which were reported by Escuer^{2a} and Soeckli-Evans⁷ are illustrative examples of the second ones. The ability of the 2,5-dpp ligand to mediate weak magnetic interactions between Cu^{II} ions when adopting a bis-bidentate coordination mode has been investigated by some of us.^{2b,8}

A series of mononuclear heteroleptic cyanide complexes of general formula $XPh_4[M^{III}(AA)(CN)_4]$ [$M = Cr, Fe$ and Co ; $X = P$ and As ; $AA =$ bidentate ligand] have been used as metalloligands for metal assembling affording nD ($n = 0-3$) heterometallic compounds with interesting magnetic properties.⁹⁻¹² The rational design of cyanide-bridged Fe^{III}-Co^{II} ribbon-like motifs with slow relaxation of the magnetization (referred to as Single Chain Magnets) being one of most appealing results obtained through this strategy.^{11a-c,13} The preparation of dinuclear cyanide-bearing precursors with a bis-bidentate ligands instead of the bidentate AA would open new avenues towards novel heterometallic species. This strategy was nicely illustrated by Herrera *et al.* in a report where the authors prepared the 3D lattice by using the $[Ru^{II}(CN)_4(\mu-bpym)]^{4-}$ precursor ($bpym = 2,2'$ -bipyrimidine) as metalloligand towards $[Gd^{III}(hfac)_3(H_2O)_2]$ ($Hhfac =$ hexafluoroacetylacetonate).¹⁴

Having this in mind, and taking advantage of the potential bis-bidentate character of the 2,5-dpp molecule, we prepared the first dinuclear 3d-cyanide building block with 2,5-dpp of formula $(PPh_4)_2[Co^{III}_2(\mu-2,5-dpp)(CN)_8] \cdot 2H_2O$ (**1**) ($PPh_4^+ =$ tetraphenylphosphonium cation) and used it as a metalloligand towards $[Mn^{II}(MAC)(H_2O)_2] \cdot 4H_2O$ ^{15,16} to afford the heterobimetallic coordination polymer $[Mn^{II}(MAC)(\mu-NC)_2Co_2^{III}(\mu-2,5-dpp)(CN)_6]_n \cdot 7nH_2O$ (**2**), [$MAC = 2,13$ -dimethyl-3,6,9,12,18-pentaazabicyclo-[12.3.1]octadeca-1(18),2,12,14,16-pentaene] (see Scheme 2). Herein we report the preparation and X-ray structures of **1** and **2** together with the cryomagnetic study of **2**.



Scheme 2. Structure and atom numbering scheme for MAC.

Experimental

All reagents and solvents were purchased from commercial suppliers and used without further purification. The organic 2,5-dpp ligand and the $[Mn(MAC)(H_2O)_2]Cl_2 \cdot 4H_2O$ complex were prepared according to the literature.^{2b,15}

Caution! Cyanides are highly toxic and should be handled with great caution. We worked at the mmol scale and the preparations were performed in a well-ventilated hood. Concentrated aqueous solutions of sodium hypochlorite and sodium hydroxide were used to transform the cyanide from the waste into cyanate.

Synthesis of $(PPh_4)_2[Co_2(\mu-2,5-dpp)(CN)_8] \cdot 2H_2O$ (**1**)

A methanolic solution (20 mL) of 2,5-dpp (0.292 g, 1.25 mmol) was poured into an aqueous solutions (20 mL) of $Co(NO_3)_2 \cdot 6H_2O$ (0.595 g, 2.5 mmol) under continuous stirring for 10 minutes, to form an orange solution. Then, an aqueous solution (10 mL) of KCN (0.528 g, 8 mmol) was added dropwise under stirring. The green suspension initially formed turned into a clear yellow solution in a few minutes. The addition of solid Ph_4PCl (0.748 g, 2.5 mmol) caused the precipitation of complex **1** as a yellow polycrystalline solid. It was collected by filtration and its recrystallization from a $H_2O:CH_3OH$ (1:10 v/v) solvent mixture in a hood afforded X-ray quality crystals of **1** as pale yellow blocks. Yield: ca. 55%. Anal. calc. for $C_{70}H_{54}Co_2N_{12}O_2P_2$ (**1**): C, 65.94; H, 4.27; N, 13.18. Found: C, 66.08; H, 4.96; N 13.04%. IR (KBr/cm^{-1}): 3432(vs), 2922(m), 2130(s), 1624(m), 1585(m), 1438(s), 1109(s), 786(m), 759(s), 690(m), 528(s).

Synthesis of $[Mn^{II}(MAC)(\mu-NC)_2Co_2^{III}(\mu-2,5-dpp)(CN)_6]_n \cdot 7nH_2O$ (**2**)

A solution of 127 mg **1** dissolved in 15 mL of a methanol:water (5:1 v/v) solvent mixture was introduced in a test tube. Then, a methanolic solution (10 mL) of $[Mn(MAC)(H_2O)_2]Cl_2 \cdot 4H_2O$ (51 mg, 0.1 mmol) was layered over it and the tube was covered with parafilm. X-ray quality crystals of **1** were obtained after three weeks under ambient conditions. Yield: ca. 60%. Anal. calcd. for $C_{37}H_{47}Co_2N_{17}MnO_7$ (**2**): C, 43.80; H, 4.67; N, 23.47. Found: C, 43.19; H, 4.16; N, 23.14%. IR (KBr/cm^{-1}): 3463(m), 2924(w), 2139(s), 1649(s), 1441(s), 1198(m), 787(m).

Physical measurements

Elemental analyses (C, H, N) were performed by the Servicio de Microanálisis from the Universidad Autónoma de Madrid. The values of the Co:P (**1**) and Co:Mn (**2**) molar ratios (1:1 and 2:1, respectively) were determined by electron microscopy at the Servicio Interdepartamental de la Universidad de Valencia. FTIR spectra ($4000-300\text{ cm}^{-1}$) were recorded on a Bruker FS55 spectrophotometer on samples of **1** and **2** prepared as KBr pellets. Variable-temperature (1.9-300 K) magnetic susceptibility measurements on a polycrystalline sample of **2** were carried out with a SQUID susceptometer using applied magnetic fields of 1 T ($T \leq 50$ K) and 500 G ($T < 50$ K). Magnetization versus magnetic field measurements of **2** were performed at 2.0 K in the field range 0-5 T. Diamagnetic corrections for the constituent atoms were made by using the Pascal's constants. The magnetic data were also corrected for the magnetization of the sample holder (a plastic bag).

X-ray data collection and structure refinement

X-ray diffraction data on single crystals of **1** and **2** were collected at room temperature with a Bruker-Nonius X8-APEXII CCD area detector system by using graphite-monochromated Mo-K α radiation ($\lambda = 0.71073 \text{ \AA}$). The data were processed through the SAINT¹⁷ reduction and SADABS¹⁸ absorption software. A summary of the crystallographic data and structure refinement for the two compounds is given in Table 1. The structures were solved by direct methods and subsequently

completed by Fourier recycling using the *SHELX*-2013 software package,¹⁹ then refined by the full-matrix least-squares refinements based on F^2 with all observed reflections. All non-hydrogen atoms of **1** and **2** except the oxygen atoms of the seven water molecules of crystallization in **2** were refined anisotropically. The latter were found disordered, as revealed by the high thermal factors; ten sites were compatible with the presence of water molecules of crystallization, only four of them being refined with full occupancy (half occupancy was assigned to the remaining six ones). All the hydrogen atoms of the 2,5-dpp ligand (**1** and **2**), the tetraphenylphosphonium cation (**1**) and the MAC ligand (**2**) were set in calculated positions and refined isotropically using the riding model. Hydrogen atoms of the uncoordinated water molecules in both **1** and **2** were neither found nor calculated. Note that there is a discrepancy between the IUPAC nomenclature given for the MAC ligand in the Introduction and the labelling scheme used for **2** when refining the structure, for convenience reasons. The final geometrical calculations and graphical manipulations were performed using the Diamond program.²⁰ Crystallographic data have been deposited at the Cambridge Crystallographic Data Centre and have been assigned CCDC reference numbers 1892383 (**1**) and 1892384 (**2**).

Table 1. Crystal data and structure refinement for compounds **1** and **2**

	1	2
Formula	C ₇₀ H ₅₄ Co ₂ N ₁₂ O ₂ P ₂	C ₃₇ H ₄₇ Co ₂ MnN ₁₇ O ₇
F_w	1275.05	1014.71
Crystal system	Monoclinic	Triclinic
Space group	$P2_1/c$	$P-1$
$a/\text{\AA}$	9.0615(2)	11.3470(11)
$b/\text{\AA}$	25.7607(5)	13.0729(12)
$c/\text{\AA}$	13.9161(3)	17.5444(16)
α°	90	90.907(4)
β°	105.6720(10)	102.483(4)
γ°	90	110.635(4)
$V/\text{\AA}^3$	3127.68(11)	2365.9(4)
Z	2	2
$D_c/\text{g cm}^{-3}$	1.354	1.424
T/K	293(2)	296(2)
μ/mm^{-1}	0.638	1.019
$F(000)$	1316	1046
Refl. collected	123588	44741
Refl. indep. [$R(\text{int})$]	7525 [0.0508]	8900 [0.0391]
Data/restraints/param.	7525 / 0 / 397	8900 / 173 / 544
Goodness-of-fit on F^2 (S) ^c	1.077	1.069
Final R indices ^{a,b}	$R_1 = 0.0380$,	$R_1 = 0.0525$,
$[I > 2\sigma(I)]$	$wR_2 = 0.0870$	$wR_2 = 0.1632$
R indices (all data)	$R_1 = 0.0504$,	$R_1 = 0.0639$,
	$wR_2 = 0.0936$	$wR_2 = 0.1732$
$\Delta\rho_{\text{max,min}}/\text{e \AA}^{-3}$	0.319 / -0.303	1.100 / -0.474

^a $R_1 = \sum ||F_o| - |F_c|| / \sum |F_o|$. ^b $wR_2 = \{[\sum w(F_o^2 - F_c^2)^2 / \sum w(F_o^2)^2]\}^{1/2}$ and $w = 1/[\sigma^2(F_o)^2 + (mP)^2 + nP]$ with $P = (F_o^2 + 2F_c^2)/3$, $m = 0.0386$ (**1**) and 0.0997 (**2**), and $n = 1.2291$ (**1**) and 2.1948 (**2**). ^c $S = [\sum w(|F_o| - |F_c|)^2 / (N_o - N_p)]^{1/2}$.

Results and discussion

View Article Online
DOI: 10.1039/C9NJ00420C

Syntheses and infrared spectroscopy

The binuclear octacyanido building block, $(\text{PPh}_4)_2[\text{Co}^{\text{III}}_2(\mu-2,5\text{-dpp})(\text{CN})_8] \cdot 2\text{H}_2\text{O}$, (**1**), was obtained through the same, simple, one-pot synthetic method, used by us to prepare the Co^{III} mononuclear cyanido complexes, $\text{PPh}_4[\text{Co}^{\text{III}}\text{L}(\text{CN})_4] \cdot n\text{S}$,^{12a,b} (L = ethylenediamine (en), 2-(aminomethyl)pyridine (ampy), 1,10-phenanthroline (phen) and 4,4'-dimethyl-2,2'-bipyridine (4,4'-dmbipy)) changing only the molar ratio between the metal cation and the ligand ($\text{Co}^{2+}:2,5\text{-dpp} = 2:1$ molar ratio). The aerial oxidation of cobalt(II) to cobalt(III) in the presence of the cyanide and 2,5-dpp groups, which are strong field ligands, accounts for the obtaining of the $\text{Co}(\text{III})$ dinuclear complex from a $\text{Co}(\text{II})$ salt.^{12a} Further, the $[\text{Co}^{\text{III}}_2(\mu-2,5\text{-dpp})(\text{CN})_8]^{2-}$ complex anion was reacted with $[\text{Mn}(\text{MAC})(\text{H}_2\text{O})_2]^{2+}$, a complex cation known as a stable species with two labile *trans* positions that can be easily replaced with organic donors^{16e} and metalloligands.^{16a-d,f,i} The reaction afforded the neutral chain **2**, $[\text{Mn}^{\text{II}}(\text{MAC})(\mu\text{-NC})_2\text{Co}_2^{\text{III}}(\mu-2,5\text{-dpp})(\text{CN})_6]_n \cdot 7n\text{H}_2\text{O}$, in which the $[\text{Co}_2(\mu-2,5\text{-dpp})(\text{CN})_8]^{2-}$ spacers connect the $[\text{Mn}(\text{MAC})]^{2+}$ nodes, the binuclear octacyanido species acting as a metalloligand toward the complex cations.

The infrared spectrum for **1** shows a strong intensity band at 2130 cm^{-1} (Fig. S1, ESI⁺) which is assigned to the terminal cyanide groups (triple carbon-nitrogen bond stretching). This value agrees with those from the literature for cyanide groups terminally bound to cobalt(III).^{12a,b,21} This band is shifted to higher wavenumbers in the infrared spectrum of **2** (Fig. S2, ESI⁺), at 2140 cm^{-1} and has a shoulder at 2160 cm^{-1} , being assigned to terminal and bridging cyanide ligands.^{12b} The strong IR peaks at 786 , 724 , 690 and 528 cm^{-1} present in **1** that are absent in **2** suggest the presence of the PPh_4^+ cations in the former compound. Finally, the shift towards higher wavenumbers of the $\nu(\text{C}=\text{N})$ and $\nu(\text{C}=\text{C})$ stretching of 2,5-dpp in **1** (1624 and 1585 cm^{-1}) and **2** (1649 and 1580 cm^{-1}) support the coordination of this molecule to the metal atoms in these compounds. All these spectroscopic features are confirmed by the X-ray structures (see below).

Description of the crystal structures

The structure of **1** consists of tetraphenylphosphonium cations, dinuclear $[\text{Co}_2^{\text{III}}(\mu-2,5\text{-dpp})(\text{CN})_8]^{2-}$ complex anions and water molecules of crystallization. **1** crystallizes in the monoclinic system as $P2_1/c$ with half of the complex anion (the second half being generated by the crystallographic inversion center), one tetraphenylphosphonium cation and one uncoordinated water molecule in the asymmetric unit, (see Fig. 1). Selected bond lengths and angles for **1** are listed in Table S1 in ESI⁺.

Each cobalt(III) cation is six-coordinate with one pyrazine and one pyridyl nitrogen atoms from the 2,5-dpp ligand and four carbon-cyanide atoms building a distorted octahedral surrounding. The two nitrogen atoms from the chelating 2,5-dpp ligand and two cyanide groups occupy the equatorial sites, while the axial positions are filled by the two remaining cyanide groups.

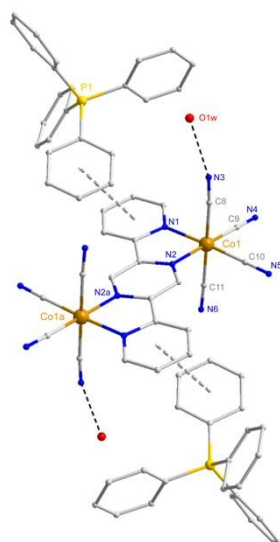


Figure 1. A view of the $[\text{Co}_2^{\text{III}}(\mu\text{-2,5-dpp})(\text{CN})_8]^{2-}$ complex anion of **1**, also showing its immediate water and tetraphenylphosphonium cations surrounding. Hydrogen bonds and $\pi\text{-}\pi$ stacking interactions are shown as black and pale grey dashed lines, respectively. Labels are added on selected atoms of the asymmetric unit only and the hydrogen atoms were omitted for clarity [Symmetry code: (a) = $-x, -y, -z$].

The reduced bite angle of the 2,5-dpp molecule [$82.12(6)^\circ$ for N1-Co1-N2] is the main reason for the distortion of the octahedral environment. The Co-C bond lengths vary from 1.866(2) to 1.908(2) Å and the Co-N bonds are larger, averaging at 1.963(1) Å. The bond lengths and angles at the cobalt(III) ion are very close to those of the tetracyanido-cobalt(III) species reported to date.^{12a,b,21} The Co-C-N_{cyanide} angles are almost

straight [$175.6(2)$ to $178.71(17)^\circ$]. The intramolecular cobalt...cobalt separation through the bridging 2,5-dpp molecule is 6.6536(4) Å.

The water molecules of crystallization in **1** are confined into a hydrophobic space and are terminally H-bonded to one of the two axial cyanide groups at each Co^{III} site [$\text{O1w}\cdots\text{N3} = 2.874(4)$ Å], this interaction contributing to the stabilization of the structure. Both the complex anions and the tetraphenylphosphonium cations form, instead, extended networks by means of several moderate-to-weak non-covalent interactions. The $[\text{Co}_2^{\text{III}}(\mu\text{-2,5-dpp})(\text{CN})_8]^{2-}$ anions, in particular, line-up through double C-H...N type of interactions [$\text{C4b-H4b}\cdots\text{N5} = 2.38$ Å; symmetry code: (b) = $x-1, y, z$] involving the outer pyridyl rings of the 2,5-dpp ligand and a Co^{III} -equatorially bound cyanide group of an adjacent molecular anion along the crystallographic *a* axis (see Fig. 2a). Weak C-H...N type interactions [$\text{C1c-H1c}\cdots\text{N4} = 2.65$ Å; (c) = $-x, -y, -z+1$] interconnecting the molecular anions along the crystallographic *c* axis do also exist, generating supramolecular anionic layers growing parallel to the *ac* plane (Fig. 2a). Similarly, the tetraphenylphosphonium cations in **1** arrange beautifully in a row through uncommon, concerted edge-to-face phenyl embraces²² involving three of the four phenyl rings along the crystallographic *c* axis (Figs. 2b), with C-H...ring centroid distances ranging from 3.33 to 3.41 Å. The fourth phenyl ring is responsible for the interconnection of such 1D motifs along the crystallographic *a* axis, with a C-H...ring centroid distance of about 3.01 Å.

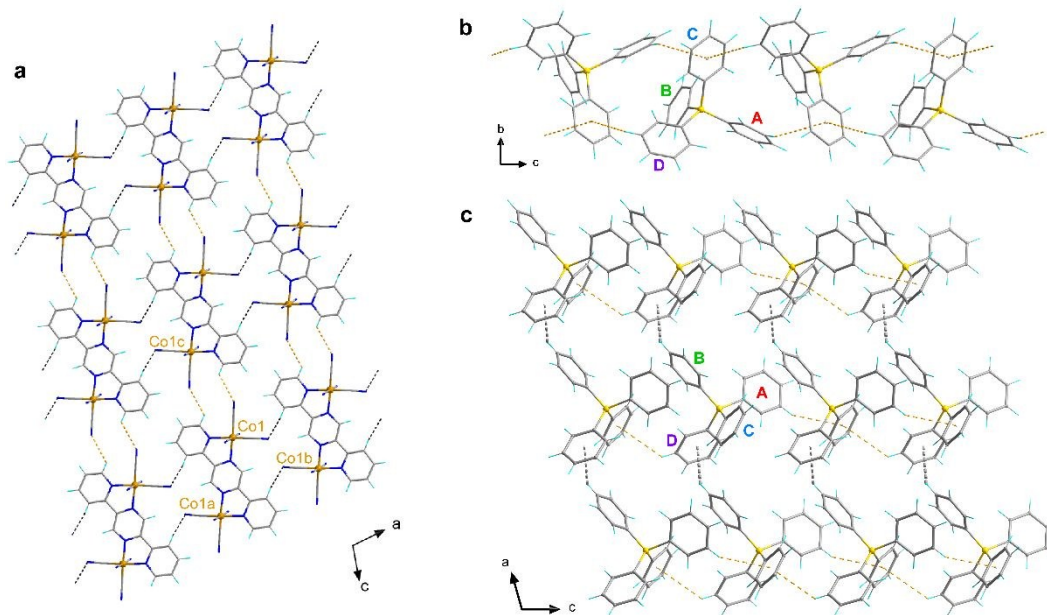


Fig. 2. (a) View of adjacent 1D motifs built by vicinal $[\text{Co}_2^{\text{III}}(\mu\text{-2,5-dpp})(\text{CN})_8]^{2-}$ anions in **1** through C-H...N contacts (black dashed lines) along the crystallographic *a* axis. Yellow dashed lines indicate weaker C-H...N interactions along the crystallographic *c* axis, leading to supramolecular anionic layers growing parallel to the *ac* plane in **1**. (b) View of the 1D motif along the crystallographic *c* axis built by edge-to-face phenyl embraces between vicinal tetraphenylphosphonium cations in **1**. Dashed lines indicate the phenyl rings involved in the embracing (A, C and D). (c) A view of the supramolecular cationic layer growing parallel to the *ac* plane, arising from the combination of the tetraphenylphosphonium phenyl embracing along the *c* axis together with multiple C-H... π interactions along the *a* axis in **1**, the latter involving phenyl rings B and D.

Published on 22 March 2019. Downloaded by Maastricht University on 04/04/2019 12:31:46 PM.

ARTICLE

The combination of the tetraphenylphosphonium phenyl embraces along the *c* axis with multiple C-H... π interactions along the *a* axis gives rise to supramolecular cationic layers growing parallel to the crystallographic *ac* plane in **1** (Fig. 2c). Thus, both anionic and cationic supramolecular layers extending in the crystallographic *ac* plane are present in **1**, and they alternate along the *b* axis (Fig. 3). Interconnections between the extended anionic and cationic portions of the crystal packing of **1** are provided by weak π - π stacking between the outer pyridyl rings of the 2,5-dpp ligand of the complex anions and a phenyl group of the tetraphenylphosphonium cations, the centroid-to-plane distances averaging at 3.72 Å and the dihedral angle between the rings being 19.3° (see Figs. 1 and 3).

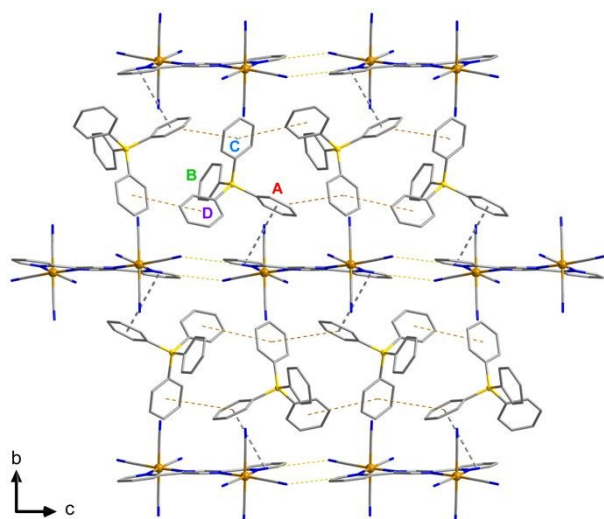


Fig. 3. Eclipsed view of a fragment of the crystal packing of **1** along the crystallographic *a* axis, showing anionic and cationic layers intercalating each other in the direction of the *b* axis, and being interconnected through π - π stacking between the 2,5-dpp ligand and the tetraphenylphosphonium cations (grey dashed lines). Hydrogen atoms and water molecules of crystallizations are omitted for clarity. Yellow and orange dashed lines indicate non-covalent interactions relevant to the development of anionic and cationic layers, respectively (see also Figs. 1-2). The four phenyl rings (noted A, B, C and D) on the cation are defined as in Figs. 2b-c.

Compound **2** crystallizes in the triclinic space group *P*-1. Its structure consists of neutral zig-zag chains of general formula $[\text{Mn}^{\text{II}}(\text{MAC})(\mu\text{-NC})_2\text{Co}_2^{\text{III}}(\mu\text{-2,5-dpp})(\text{CN})_6]_n \cdot 7n\text{H}_2\text{O}$ running along the crystallographic *b* axis. The asymmetric unit comprises a $[\text{Mn}^{\text{II}}(\text{MAC})]^{2+}$ cationic moiety connected to a $[\text{Co}_2^{\text{III}}(\mu\text{-2,5-dpp})(\text{CN})_6]^{2-}$ anionic fragment through a cyanido bridge [C19-N9], plus the seven water molecules of crystallization tentatively distributed over ten sites of which six with half occupancy (Fig. 4a-b). It is worth to mention that the exact

water content in **2** could not be determined and the declared value represents our best estimate based on all data in hand (elemental analyses, magnetism, crystallography). The further development of the chain is determined by a second cyanido group [C15-N5] belonging to the dicobalt(III) metalloligand which coordinates to an adjacent Mn^{II} metal ion. A fragment of the heterobimetallic alternating $\text{Co}^{\text{III}}\text{-Mn}^{\text{II}}$ chain of **2** is shown in Fig. 4c, while selected bond distances and angles for this compound are listed in Table S2 in ESI†. Each Mn^{II} ion is confined within the pentadentate macrocyclic MAC ligand and it is seven-coordinate: five in-plane nitrogen atoms from the MAC ligand (N13, N14, N15, N16 and N17 set of atoms) and two axial cyanido nitrogen atoms from two dicobalt(III) units build a distorted pentagonal bipyramidal environment around the manganese atom (see Fig. 4). The two cyanido bridges at the manganese side are bent, the values of the Mn-N-C angles being 159.0(3) and 161.1(3)° at N9 and N5a, respectively. The Mn-N_{cyanido} bond lengths [mean value 2.275(4) Å] are shorter than the Mn-N_{imine} [Mn1-N14 and Mn1-N15, averaging at 2.302(4) Å] and the Mn-N_{amino} [Mn1-N16 and Mn1-N17, averaging at 2.297(4) Å] distances, but longer than the Mn-N_{pyridyl} bond length [Mn1-N13 = 2.210(2) Å]. These structural pattern regarding the Mn^{II} environment in **2** agrees with those observed in previous structures containing the $\{\text{Mn}^{\text{II}}(\text{MAC})\}^{2+}$ fragment.¹⁶

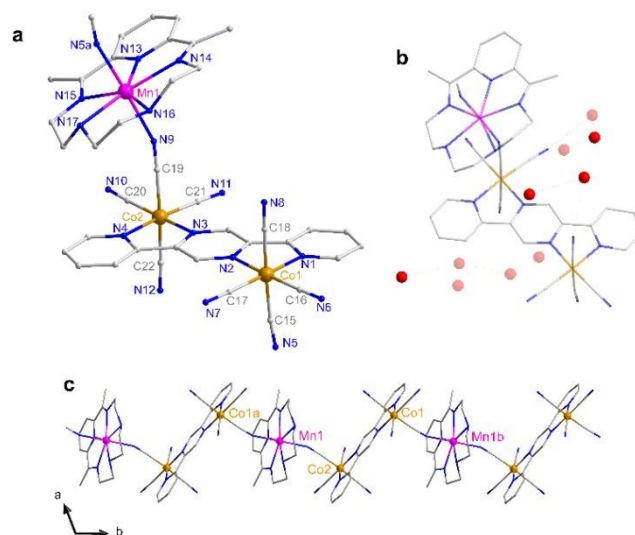


Fig. 4. (a) Perspective view of the repeating unit of the heterobimetallic alternating $\text{Co}^{\text{III}}\text{-Mn}^{\text{II}}$ chain of **2**. (b) View of the asymmetric unit, comprising the fragment shown in (a) and the seven disordered water molecules of crystallization occupying ten different sites with either full (dark red spheres) or half occupancy (light red spheres). (c) View of a fragment of the chain running along the crystallographic *b* axis. Labels are put on selected atoms only. Hydrogen atoms are not shown for clarity [Symmetry codes: (a) = $x, y-1, z$; (b) = $x, y+1, z$.]

As in **1**, the two cobalt(III) ions in **2** are six-coordinate in an octahedral environment formed by two nitrogen atoms belonging to the bridging 2,5-dpp ligand and four cyanide-carbon atoms. The bite angles of the bis-chelating 2,5-dpp molecule are 82.14(11) and 81.98(11)° at Co2 and Co1

respectively, values which are very close to the corresponding bite angle in **1**. The Co-C_{cyanido} bond lengths have values in the range 1.865(3)-1.900(4) (at Co1) and 1.871(4)-1.905(4) Å (at Co2), while the Co-N_{2,5-dpp} distances are generally longer [mean values 1.970(3) (at Co1) and 1.971(3) Å (at Co2)].

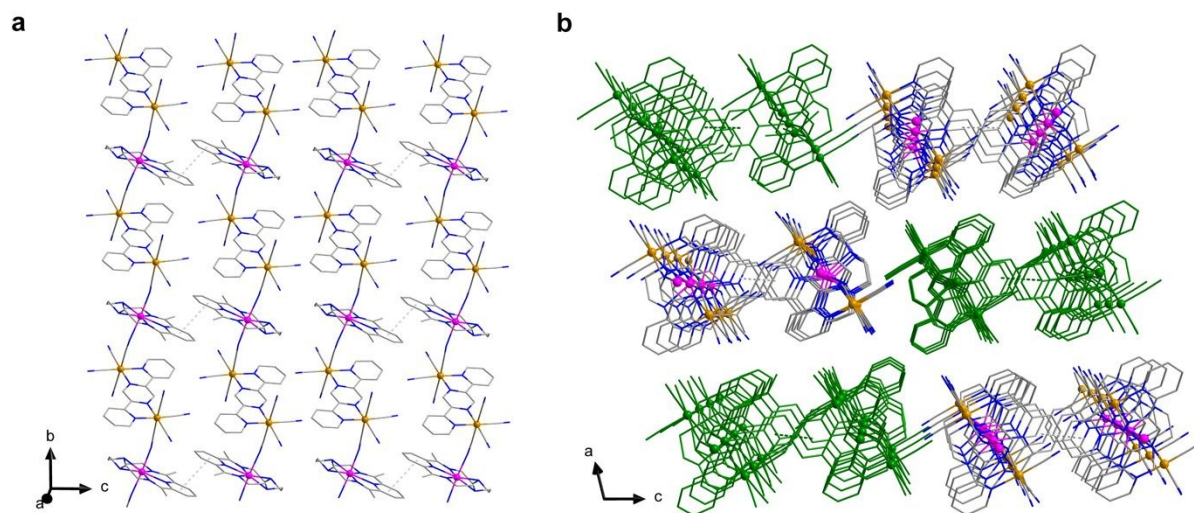


Fig. 5. (a) View of fragments of vicinal heterometallic chains in the *bc* plane in **2**, coupled into stripes by means of face-to-face π - π stacking interactions involving the pyridyl ring of the MAC ligand (grey dashed lines). (b) A view of the crystal packing of **2** along the crystallographic *b* axis, showing the arrangement of vicinal supramolecular stripes in the *ac* plane, some of which being highlighted in green for clarity. Hydrogen atoms and water molecules of crystallization are omitted for clarity.

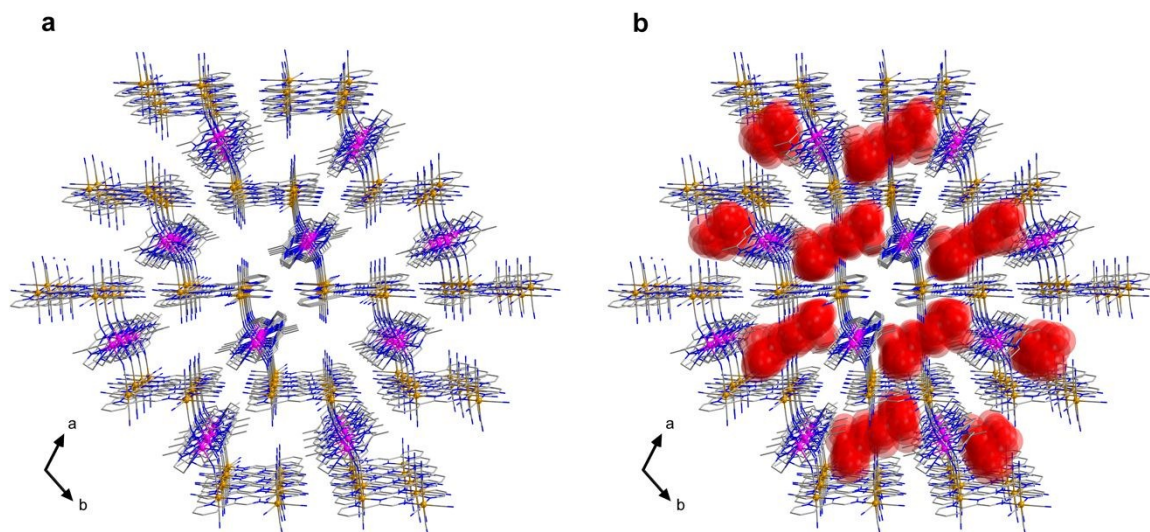


Fig. 6. (a) Perspective view of a fragment of the crystal packing of **2** along the crystallographic *c* axis, showing in (b) the disordered water molecules (van der Waals model) filling the channels which develop in the same direction.

The values of the Co-C-N_{cyanide} angles are close to linearity [with values varying in the ranges 174.9(3)-178.9(4)° for Co1 and 175.7(3)-178.0(5)° for Co2]. Bond distances and angles within the cyanido-bearing Co^{III} fragments (see Table S2 in ESI[†]), are in agreement with those observed in **1**.

The shortest Co^{III}...Mn^{II} separation across the bridging cyanide is 5.2178(8) Å, while the Co^{III}...Co^{III} separation through the bridging 2,5-dpp ligand is 6.6824(8) Å, a value very similar to that observed in **1**. The intrachain Mn^{II}...Mn^{II} separation is 13.0729(12) Å whereas the shortest interchain Mn^{II}...Mn^{II}

distance is 8.5873(13) Å. The intrachain angles between the metal ions are almost right [Co1-Co2-Mn1 = 98.381(12)° and Mn1b-Co1-Co2 = 96.076(12)°; symmetry code: (b) = *x*, -1+*y*, *z*] or straight [Co1a-Mn1-Co2 = 175.408(13)°].

Two chains are coupled into a stripe by means of face-to-face, parallel by symmetry, π - π stacking interactions involving the pyridyl ring of neighboring MAC ligands (Fig. 5), whose interplanar distance is about 3.39 Å. Such stripes are closely packed in the crystallographic *ac* plane, however no further relevant π - π stacking, C-H... π or C-H...N interactions can be

noted. Rather, viewed along the crystallographic *c* axis, the 3D packing of **2** reveals the presence of small channels, where all the disordered lattice water molecules are located (Fig. 6), and they are involved into an extensive network of hydrogen bonds which contribute to the stabilization of the crystal packing.

Magnetic properties

Compound **1** is a diamagnetic species as expected for a dicobalt(III) complex where each metal centre is six-coordinated by four strong field cyanide ligands and one pyridyl and one pyrazine nitrogen atoms from a bis-bidentate 2,5-dpp molecule. The magnetic properties of **2** in the form of $\chi_M T$ versus *T* plot [χ_M is the magnetic susceptibility per $\text{Co}^{\text{III}}_2\text{Mn}^{\text{II}}$ unit] are shown in Fig. 7. At room temperature, $\chi_M T$ for **2** is ca. $4.38 \text{ cm}^3 \text{ mol}^{-1} \text{ K}$, a value which is as expected for a magnetically isolated high-spin Mn^{II} with $g_{\text{Mn}} = 2.0$, the Co^{III} being diamagnetic. Upon cooling, this value remains constant until 10 K and it further exhibits a very small decrease to $4.22 \text{ cm}^3 \text{ mol}^{-1} \text{ K}$ at 1.9 K. This behaviour corresponds to a practically magnetically isolated spin sextet with a *g* value of 2.005(3).

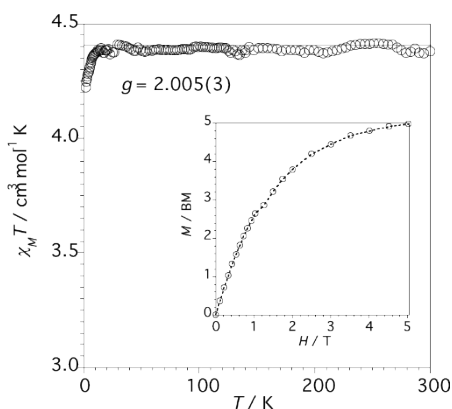


Fig. 7. Plot of $\chi_M T$ vs. *T* for **2**: (o) experimental; (—) best-fit curve through a Curie law (see text). The inset shows the thermal dependence of the magnetization for **2** at 2.0 K. The dashed line corresponds to the Brillouin function for a magnetically isolated $S = 5/2$ with $g = 2.005$.

This is corroborated by the field dependence of the magnetization (*M*) of **2** at 2.0 K, *M* at 5 T tending to a value of 5.0 BM (see inset of Fig. 7).

Conclusions

The first heterobimetallic 3d cyanido complex was obtained and crystallographically characterized: a one pot reaction under ambient conditions, involving the 2,5-dpp organic molecule, cobalt(II) ions and cyanide anions affords the octacyanido complex $(\text{Ph}_4\text{P})_2[\text{Co}_2^{\text{III}}(\mu\text{-}2,5\text{-dpp})(\text{CN})_8]\cdot 2\text{H}_2\text{O}$ (**1**) where the 2,5-dpp molecule acts as a bis-bidentate ligand and the cobalt(II) ion has become cobalt(III) by air oxidation. This cyanido building-block was used as a metalloligand towards the $[\text{Mn}(\text{MAC})(\text{H}_2\text{O})_2]^{2+}$ complex cation to construct a heterometallic chain, $[\text{Mn}^{\text{II}}(\text{MAC})(\mu\text{-NC})_2\text{Co}_2^{\text{III}}(\mu\text{-}2,5\text{-dpp})(\text{CN})_6]_n \cdot 7n\text{H}_2\text{O}$. This result proves the ability of the cyanide-bearing cobalt(III) precursor to act as an efficient spacer

towards the peripheral cyanide groups. Being a robust diamagnetic species, complex **1** opens a new avenue for metal assembling in the near future when used as a metalloligand versus either preformed metal complexes whose coordination sphere is unsaturated or well fully solvated metal ions.

Conflicts of interest

There are no conflicts to declare.

Acknowledgements

This work was financially supported by the Romanian National Authority for Scientific Research (CNCS-UEFISCDI) (Projects PN-II-RU-TE-2014-4-1556 and PN-III-P1-1.1-MC-2018-1877), the Italian Ministero dell'Istruzione dell'Università e della Ricerca (MIUR) and the Ministerio Español de Economía y Competitividad (MINECO) (Project CTQ2016-75068P and Unidad de Excelencia María de Maetzu MDM-2015-0538).

Notes and references

- (a) C. R. K. Glasson, L. F. Lindoy and G. V. Meehan, *Coord. Chem. Rev.*, 2008, **252**, 940-963; (b) L. Salassa, *Eur. J. Inorg. Chem.*, 2011, 4931-4947; (c) R. D. Hancock, *Chem. Soc. Rev.*, 2013, **42**, 1500-1524; (d) S. Culham, P.-H. Lanoë, V. L. Whittle, M. C. Durrant, J. A. Gareth Williams and V. N. Kozhevnikov, *Inorg. Chem.*, 2013, **52**, 10992-11003; (e) B. Colasson, A. Credi and G. Ragazzon, *Coord. Chem. Rev.*, 2016, **325**, 125-134; (f) B. Floris, M. P. Donzello, C. Ercolani and E. Viola, *Coord. Chem. Rev.*, 2007, **347**, 115-140; (g) M. Attwood and S. S. Turner, *Coord. Chem. Rev.*, 2017, **353**, 247-277; (h) V. Bravec and J. Kasatkova, *Coord. Chem. Rev.*, 2018, **376**, 75-94; (i) A. M.-H. Yip and K. K.-W. Lo, *Coord. Chem. Rev.*, 2018, **361**, 138-163; (j) A. P. Sadimenko and O. O. Okoh, *Adv. Heterocyclic Chem.*, 10.1016/bs.aihch.2018.06.001.
- (a) A. Escuer, T. Comas, R. Vicente and J. Ribas, *Transition Met. Chem.*, 1993, **18**, 42-44; (b) C. Yuste, A. Bentama, S.-E. Stiriba, D. Armentano, G. De Munno, F. Lloret and M. Julve, *Dalton Trans.*, 2007, 5190-5200; (c) L. Donato, C. E. McCusker, F. N. Castellano, E. Zysman-Colman, *Inorg. Chem.*, 2013, **52**, 8495-8504.
- (a) S. Serroni and G. Denti, *Inorg. Chem.*, 1992, **31**, 4251-4255; (b) A. Neels and H. Stoeckli-Evans, *Inorg. Chem.*, 1999, **38**, 6164-6170.
- M. Al-Anber, N. Wetzold, B. Walfort, T. Rüffer and H. Lang, *Inorg. Chim. Acta*, 2013, **398**, 124-131.
- E. C. Constable, H. Eriksson, C. E. Housecroft, B. M. Kariuki, E. Nordlander and J. Olsson, *Inorg. Chem. Commun.*, 2001, **4**, 749-752.
- T. Tsubomura, S. Enoto, S. Endo, T. Tamane, K. Matsumoto and T. Tsukuda, *Inorg. Chem.*, 2005, **44**, 6373-6378.
- A. Neels and H. Stoeckli-Evans, *Chimia*, 1993, **47**, 198-202.
- (a) A. Bentama, O. Schott, J. Ferrando-Soria, S.-E. Stiriba, J. Pasán, C. Ruiz-Pérez and M. Julve, *Inorg. Chim. Acta*, 2013, **389**, 52-59; (b) C. Yuste, A. Bentama, N. Marino, D. Armentano, F. Setifi, S. Triki, F. Lloret and M. Julve, *Polyhedron*, 2009, **28**, 1287-1294.
- R. Lescouëzec, L. M. Toma, J. Vaissermann, M. Verdager, F. S. Delgado, C. Ruiz-Pérez, F. Lloret and M. Julve, *Coord. Chem. Rev.*, 2005, **249**, 2691-2729; (b) M.-G. Alexandru, D. Visinescu, B. Braun-Cula, F. Lloret and M. Julve, *Eur. J. Inorg. Chem.*, 2018, 349-359; (c) M.-G. Alexandru, D. Visinescu, S. Shova, W.

ARTICLE

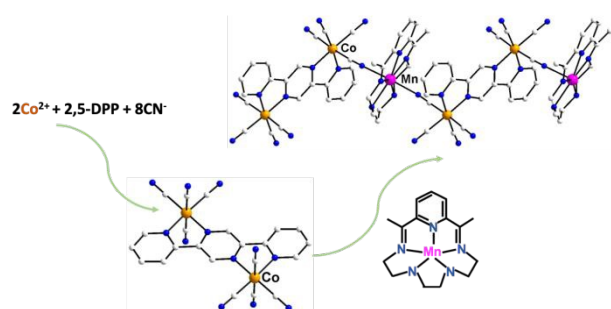
Journal Name

- X. C. Oliveira, F. Lloret and M. Julve, *Dalton Trans.*, 2018, **47**, 6005-6017.
- 10 Y.-H. Li, W.-R. He, X.-H. Ding, S. Wang, L.-F. Cui and W. Huang, *Coord. Chem. Rev.*, 2012, **256**, 2795-2815.
- 11 (a) L. M. Toma, C. Ruiz-Pérez, F. Lloret and M. Julve, *Inorg. Chem.*, 2012, **51**, 1216-1218; (b) L. M. Toma, J. Pasán, C. Ruiz-Pérez, F. Lloret and M. Julve, *Dalton Trans.*, 2012, **41**, 13716-13726; (c) L. M. Toma, C. Ruiz-Pérez, J. Pasán, W. Wernsdorfer, F. Lloret and M. Julve, *J. Am. Chem. Soc.*, 2012, **134**, 15265-15268; (d) M.-G. Alexandru, D. Visinescu, M. Andruh, N. Marino, D. Armentano, J. Cano, F. Lloret and M. Julve, *Chem. Eur. J.*, 2015, **21**, 5429-5446; (e) M.-G. Alexandru, D. Visinescu, S. Shova, M. Andruh, F. Lloret and M. Julve, *Inorg. Chem.*, 2017, **56**, 2258-2269.
- 12 (a) M.-G. Alexandru, D. Visinescu, N. Marino, G. De Munno, J. Vallejo, F. Lloret and M. Julve, *Eur. J. Inorg. Chem.*, 2014, 4564-4572; (b) M.-G. Alexandru, D. Visinescu, N. Marino, G. De Munno, F. Lloret and M. Julve, *RSC Adv.*, 2015, **5**, 95410-95420; (c) M.-G. Alexandru, D. Visinescu, S. Shova, F. Lloret and M. Julve, *Dalton Trans.*, 2017, **46**, 39-43.
- 13 (a) R. Lescouëzec, J. Vaissermann, C. Ruiz-Pérez, F. Lloret, R. Carrasco, M. Julve, M. Verdaguer, Y. Dromzée, D. Gatteschi and W. Wernsdorfer, *Angew. Chem. Int. Ed.*, 2003, **42**, 1483-1486; (b) L. M. Toma, R. Lescouëzec, J. Pasán, C. Ruiz-Pérez, J. Vaissermann, J. Cano, R. Carrasco, W. Wernsdorfer, F. Lloret and M. Julve, *J. Am. Chem. Soc.*, 2006, **128**, 4842-4853.
- 14 J.-M. Herrera, S. G. Baca, H. Adams and M. D. Ward, *Polyhedron*, 2006, **25**, 869-875.
- 15 O. Jiménez-Sandoval, D. Ramírez-Rosales, M. del Jesús Rosales-Hoz, M. E. Sosa-Torres, R. Zamorano-Ulloa, *J. Chem. Soc., Dalton Trans.* **1998**, 1551-1556.
- 16 (a) A. K. Sra, M. Andruh, O. Kahn, S. Golhen, L. Ouahab and J. V. Yakhmi, *Angew. Chem. Int. Ed.*, 1999, **38**, 2606-2609; (b) A. K. Sra, J.-P. Sutter, P. Guionneau, D. Chasseau, J. V. Yakhmi and O. Kahn, *Inorg. Chim. Acta*, 2000, **300-302**, 778-782; (c) G. Rombaut, S. Golhen, L. Ouahab, C. Mathonière and O. Kahn, *J. Chem. Soc., Dalton Trans.*, **2000**, 3609-3614; (d) S. Tanase, M. Andruh, N. Stanica, C. Mathonière, G. Rombaut, S. Golhen and L. Ouahab, *Polyhedron*, **2003**, **22**, 1315-1320; (e) C. Paraschiv, J.-P. Sutter, M. Schmidtman, A. Müller, M. Andruh, *Polyhedron*, **2003**, **22**, 1611-1615; (f) C. Paraschiv, M. Andruh, Y. Journaux, Z. Žak, N. Kyritsakas and L. Ricard, *J. Mater. Chem.*, **2006**, **16**, 2660-2668; (g) Q.-L. Wang, Y.-Z. Zhang, H. Southerland, A. V. Prosvirin, H. Zhao and K. R. Dunbar, *Dalton Trans.*, **2014**, **43**, 6802-6810; (h) K. Wang, B. Xia, Q.-L. Wang, Y. Ma, D.-Z. Liao and J. Tang, *Dalton Trans.*, **2017**, **46**, 1042-1046; (i) C. Pichon, B. Elrez, V. Béreau, C. Duhayon and J.-P. Sutter, *Eur. J. Inorg. Chem.*, **2018**, 340-348.
- 17 SAINT, version 6.45, Bruker Analytical X-ray Systems, Madison, WI, 2003.
- 18 G. M. Sheldrick. SADABS Program for Absorption Correction, version 2.10, Analytical X-ray Systems, Madison, WI, 2003.
- 19 (a) G. M. Sheldrick, *Acta Crystallogr.*, 2015, **C71**, 3-8; (b) G. M. Sheldrick, *Acta Crystallogr.*, 2008, **A64**, 112-122; (c) SHELXTL-2013/4, Bruker Analytical X-ray Instruments, Madison, WI, 2013.
- 20 Diamond - Crystal and Molecular Structure Visualization. Crystal Impact - Dr. H. Putz & Dr. K. Brandenburg GbR, Kreuzherrenstr. 102, 53227 Bonn, Germany
- 21 G. Lyubartseva and S. Parkin, *Acta Crystallogr.*, 2010, **E66**, m475-476.
- 22 I. Dance and M. Scudder, *Chem. Eur. J.*, 1996, **2**, 481-486.

View Article Online
DOI: 10.1039/C9NJ00420C

New Journal of Chemistry Accepted Manuscript

Table of contents



The first bimetallic 3d cyanido-bearing complex with 2,5-dpp as a bridge, $(\text{Ph}_4\text{P})_2[\text{Co}_2^{\text{III}}(\mu\text{-}2,5\text{-dpp})(\text{CN})_8] \cdot 2\text{H}_2\text{O}$, is obtained and used as a metalloligand towards the $[\text{Mn}(\text{MAC})(\text{H}_2\text{O})_2]^{2+}$ cation to build a $\{\text{Co}^{\text{III}}\text{Mn}^{\text{II}}\}$ heterobimetallic chain.